CrystEngComm

COMMUNICATION

Cite this: *CrystEngComm*, 2018, **20**, 1473

Received 2nd December 2017,
Accepted 9th January 2018

DOI: 10.1039/c7ce02073b

rsc.li/crystengcomm

Formation mechanism of rod-like ZIF-L and fast phase transformation from ZIF-L to ZIF-8 with morphology changes controlled by polyvinylpyrrolidone and ethanol†

Huifen Fu,[a] Zhihua Wang,*[b] Xun Wang,[a] Peng Wang[a] and Chong-Chen Wang *[a]

Rod-like ZIF-L was formed with the aid of PVP through a self-assembly mechanism. A fast phase transformation from irregular ZIF-L to rhombic dodecahedral ZIF-8 occurred once ethanol was used as the washing solvent due to its weak crystallinity and small size. ZIFs with different coordination modes, morphologies and sizes were obtained *via* this facile method.

Metal–organic frameworks (MOFs), as a class of porous crystalline materials constructed from metal ions and organic ligands through coordination bonds, have been of great interest due to their beneficial characteristics like ultra-high surface area, well-ordered porous structure and structure designability.[1,2] Zeolitic imidazolate frameworks (ZIFs) are a kind of typical MOFs, which are constructed from tetrahedral metal ions like Zn^{2+} or Co^{2+} bridged by an imidazolate ligand.[3,4] ZIFs attracted considerable attention in many fields,[5,6] like catalysis,[7] gas separation[8,9] and gas storage,[10] due to their active sites, ultra-high surface area, and permanent porosity with uniform pore cavity size, along with high thermal and chemical stability.[11,12]

ZIF-8, as a three-dimensional (3D) framework adopting Zn^{2+} as a template, was firstly prepared by the reaction between $Zn(NO_3)_2$ and 2-methylimidazole (2-mim) in *N*,*N*-dimethylformamide (DMF).[11] Then, it was found that ZIF-8 can also be obtained in methanol or ethanol solution.[3] Lai's group reported for the first time that ZIF-8 can be synthesized in aqueous solution when the ratio of 2-mim to Zn^{2+} was increased to 70.[13] However, Zn-ZIF-L, as a two-dimensional (2D) ZIF, was formed in aqueous solution when the 2-mim/Zn^{2+} ratio was 8, as reported by Wang's group.[14] This revealed that the ratio of 2-mim/Zn^{2+} in aqueous solution heavily affects the structure of ZIFs, in which the high ratio facilitates the formation of ZIF-8 while the low ratio is beneficial to the growth of ZIF-L. In addition, a variety of synthesis routes to ZIF-8 were summarized by Ahn's group.[15]

Phase transformation from ZIF-L to ZIF-8 has been found by Wang's group.[16] They reported that a solid powder of ZIF-L could be transformed into ZIF-8 in various organic solvents at elevated temperatures or after being exposed to various organic solvent vapors for 72 h at 60 °C. The understanding of phase transformation was beneficial to studying the growth, structure and performance of ZIFs, therefore it was necessary to further investigate the phase transformation of ZIFs.

It was generally deemed that morphology control of MOFs attracted considerable attention,[17] considering that the morphology could greatly affect the corresponding performances.[18,19] In most cases, ZIF-8 presented a rhombic dodecahedral morphology.[20–22] It was reported for the first time that cetyltrimethylammonium bromide (CTAB) was selected to tune the shape and size of ZIF-8, which resulted in rhombic dodecahedral, truncated rhombic dodecahedral and truncated cubic morphologies *via* changing the CTAB amount.[23] Schneider's group[24] found that the growth of ZIF-8 in methanol evolved with time from cubes to intermediate shapes. To the best of our knowledge, most reported ZIF-L presented a leaf-like structure.[25,26] It was reported that ZIF-L and ZIF-67@ZIF-L with different morphologies were prepared by changing the volume ratio of methanol/water.[27] Chen's group[28] prepared Pd@ZIF-L with a uniform crosshair-star shape using polyvinylpyrrolidone (PVP)-modified Pd nanoparticles, and Pd@ZIF-L with different morphologies was obtained by controlling the temperature.[29] However, the formation mechanism of ZIFs was rarely reported. Within this paper, rod-like ZIF-L and ZIF-8 were prepared, then the phase transformation, morphology evolution and the corresponding mechanism were investigated in detail.

ZIF-L was obtained after the reaction between aqueous solutions of $Zn(NO_3)_2$ (1 mmol, 0.297 g) and 2-mim (10 mmol, 0.82 g) with different reaction times, as shown in Fig. 1a–c.

[a] *Beijing Key Laboratory of Functional Materials for Building Structure and Environment Remediation, Beijing University of Civil Engineering and Architecture, Beijing, 100044, China. E-mail: chongchenwang@126.com*
[b] *State Key Laboratory of Chemical Resource, Beijing University of Chemical Technology, Beijing 100029, China. E-mail: zhwang@mail.buct.edu.cn*
† Electronic supplementary information (ESI) available. See DOI: 10.1039/c7ce02073b

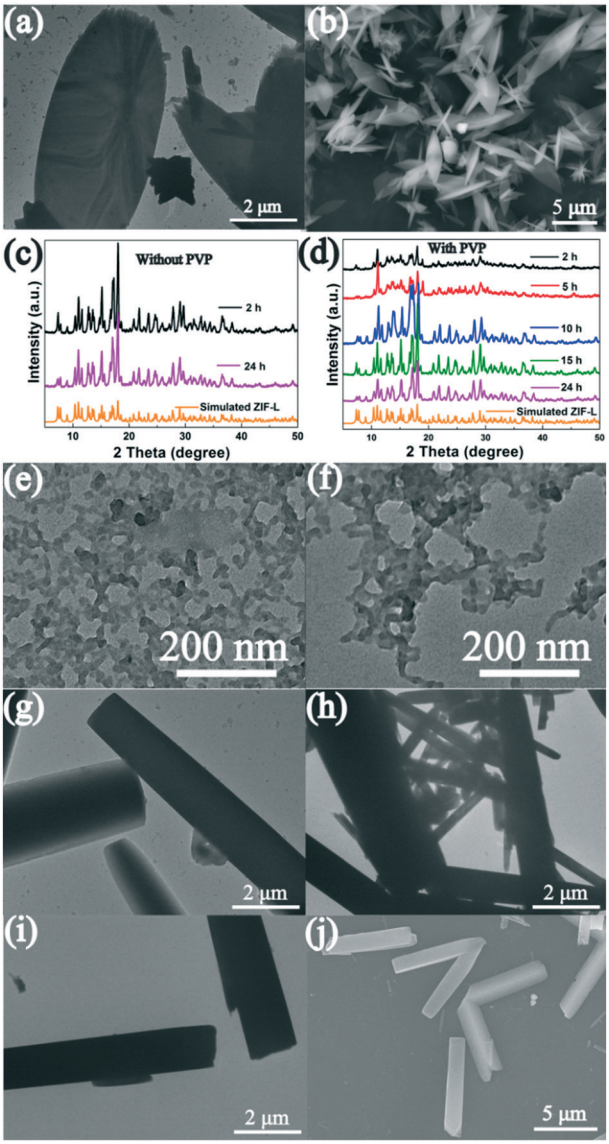

Fig. 1 (a) TEM and (b) SEM images of ZIF-L prepared without PVP when the reaction time is 2 h and 24 h. (c and d) XRD patterns of samples prepared (c) without and (d) with PVP. (e–i) TEM and (j) SEM images of ZIF-L prepared with PVP when the reaction time is (e) 2 h, (f) 5 h, (g) 10 h, (h) 15 h and (i and j) 24 h. All samples were washed with pure water.

The separation and washing of the obtained products were realized by centrifugation (8000 rpm, 10 min), and the washing step was repeated three times. When pure water was used during the washing step, incomplete leaf-like ZIF-L was obtained after 2 h (Fig. 1a and c). The sample presented leaf-like ZIF-L when the reaction time was 24 h (Fig. 1b and c), which was comparable to that reported in the literature.[31,32] The size of the ZIF-L became larger with increasing reaction time. Therefore, it can be guessed that the formation of leaf-like ZIF-L underwent nucleation and growth stages.[30]

Meanwhile, when the surfactant PVP was introduced into the aqueous solutions of $Zn(NO_3)_2$ and 2-mim (10 mmol, 0.82 g), rod-like ZIF-L was formed after 24 h (Fig. 1d, i and j). To investigate the growth mechanism of rod-like ZIF-L, samples obtained at different reaction times were collected, and the samples were defined as ZIF(2h), ZIF(5h), ZIF(10h), ZIF(15h) and ZIF(24h) when the reaction time is 2 h, 5 h, 10 h, 15 h and 24 h, respectively. It can be seen from Fig. 1d that the XRD patterns of all samples matched well with that of the simulated ZIF-L, indicating that PVP cannot affect the coordination mode between Zn^{2+} and 2-mim, but noticeably influence the morphology of ZIF-L. It is interesting to find that ZIF(2h) and ZIF(5h) presented an irregular shape (Fig. 1e and f), ZIF(10h) consisted of irregular and rod-like ZIF-L (Fig. 1g), while ZIF(15h) and ZIF(24h) exhibited rod-like ZIF-L (Fig. 1h–j). This revealed that the formation of rod-like ZIF-L followed a self-assembly mechanism.[35] From the perspective of experimental phenomena, the reaction solution turned into a milky liquid immediately after $Zn(NO_3)_2$ was added into the aqueous solution of 2-mim in the presence of PVP. When PVP was absent, the formation of the milky liquid needed a longer time (10 min). This indicated that PVP accelerated the nucleation and growth rate of ZIF-L, which might be attributed to the identical N atoms in PVP and 2-mim (Fig. S1†). A larger amount of ZIF-L nuclei was immediately formed in the presence of PVP, leading to the formation of ZIF-L with a smaller size and an irregular shape within 2 h. It was reported that PVP, as a surfactant, could be used to tune the morphology of metal oxides like CeO_2 and ZnO.[33,34] In detail, PVP could be adsorbed onto a specific lattice plane of metal oxides, limiting the growth of the lattice plane, and finally leading to the formation of metal oxides with a specific morphology. In our case, PVP could be selectively adsorbed onto a specific lattice of the irregular ZIF-L particles. As time went on, the irregular ZIF-L particles could be assembled into rod-like ZIF-L through oriented attachment.[36]

In the absence of PVP, the structure and morphology of the ZIF-L washed with ethanol were identical to that being washed with pure water, as shown in Fig. 1a–c and 2a–c. However, in the presence of PVP, rhombic dodecahedral ZIF-8 was obtained using ethanol as the washing solvent when the reaction time was 2 h (Fig. 2d and e). Therefore, it can be indicated that irregular ZIF-L and rhombic dodecahedral ZIF-8 were prepared in aqueous solution by changing the washing solvents with the aid of PVP (Fig. 1e and 2e).

It has been reported that $Zn(NO_3)_2$ reacted with 2-mim in aqueous solution to form ZIF-L when the ratio of 2-mim to $Zn(NO_3)_2$ was not very high, *i.e.* 8.[14] In our case, the ratio is 10, and ZIF-L should be formed in aqueous solution. However, ZIF-8 was formed after a washing process using ethanol as solvent. It was implied that an inter-dimensional phase transformation from ZIF-L to ZIF-8 occurred when ethanol was used during the washing process. Therefore, it can be concluded that the phase transformation should be controlled by ethanol. In addition, when the products were separated from the original reaction system, and then re-dispersed in ethanol for 30 min, rhombic dodecahedral ZIF-8 could also be formed, as shown in Fig. S2.† Phase transformation from ZIF-L to ZIF-8 occurred only when PVP existed,

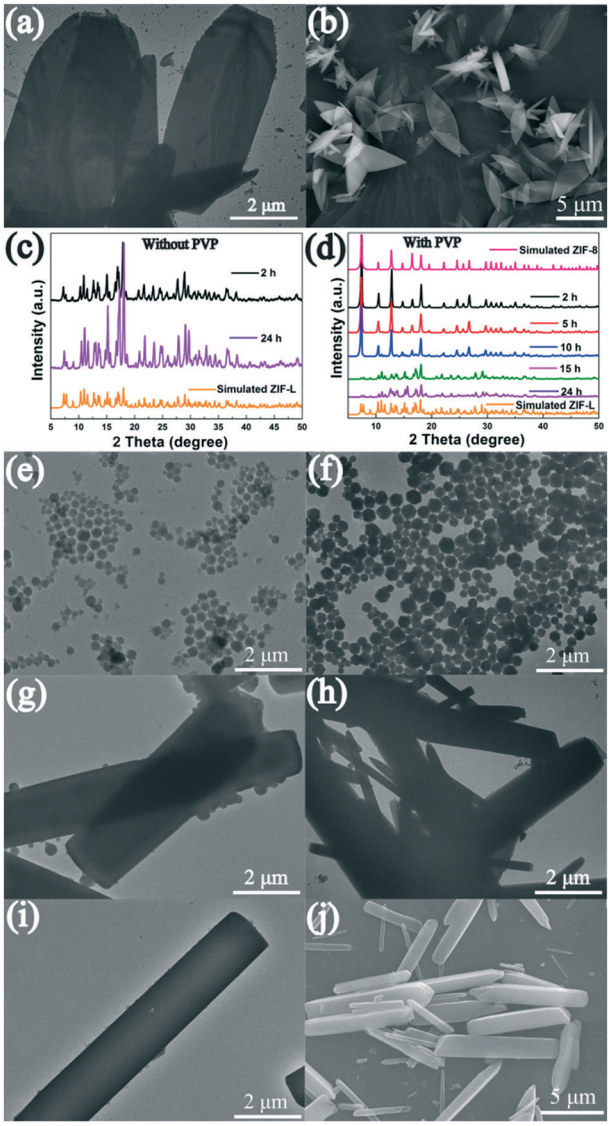

Fig. 2 (a) TEM and (b) SEM images of ZIF-L prepared without PVP when the reaction time is 2 h and 24 h. (c and d) XRD patterns of samples prepared (c) without and (d) with PVP. (e–i) TEM and (j) SEM images of ZIF-L prepared with PVP when the reaction time is (e) 2 h, (f) 5 h, (g) 10 h, (h) 15 h and (i and j) 24 h. All samples were washed with absolute ethanol.

indicating that the phase transformation was also controlled by PVP. As shown in Fig. 1e and 2e, when the reaction time was 2 h, the sizes of ZIF-L prepared with PVP were smaller than those prepared without PVP. Ethanol could control the phase transformation from ZIF-L to ZIF-8 resulting from the diffusion of ethanol molecules into the inner part of ZIF-L, in which the diffusion rate of ethanol can be heavily affected by the size of ZIF-L. A smaller size of ZIF-L along with PVP resulted in the faster diffusion of ethanol and phase transformation.

ZIF-8 and ZIF-L are both made up of the same building blocks with different topology structures.[16] ZIF-8 has a 3D skeleton structure with a sodalite (SOD) topology,[11] while ZIF-L has a 2D layered structure, in which the layers of ZIF-L were bridged by N–H···N hydrogen bonds.[37,38] It has been reported that the 2D layered network structure of ZIF-L is part of the 3D ZIFs, and the transformation from ZIF-L to 3D ZIFs can be easily understood.[39] The ZIF-L prepared with PVP would adsorb extra Zn^{2+} due to the weak interaction between Zn^{2+} and N atoms in PVP. When irregular ZIF-L prepared with PVP was re-dispersed in ethanol, the phase transformation would start, and the 2-mim with free and uncoordinated N–H in ZIF-L could further coordinate with Zn^{2+} adsorbed on PVP. Finally, the rhombic dodecahedral ZIF-8 was formed. Furthermore, in this process, the size of the particles became larger. In other words, in the presence of PVP, not only the coordination mode but also the morphology and size would change when ethanol was used in the washing step.

In addition, ZIF-8 could also be obtained using methanol and isopropanol as washing solvents when the reaction time was 2 h (Fig. S3†), indicating that methanol and isopropanol can also induce the phase transformation from ZIF-L to ZIF-8. Ethanol was selected as the preferential washing solvent due to its lower price and toxicity.

It was generally reported that complete phase transformation was observed in ethanol for 72 h at 60 °C.[16] However, in our case, complete phase transformation was achieved within an hour at room temperature. The fast transformation may be caused by the weak crystallinity of ZIF-L. It can be seen from Fig. 1d that the crystallinity of ZIF(2h) and ZIF(5h) was not good enough in the presence of PVP, which might contribute to the fast phase transformation from ZIF-L to ZIF-8 (Fig. 2d–f). With increasing reaction time, the crystallinity of ZIF-L could become better, and the size of ZIF-L would become larger. It can be speculated that the rate of the phase transformation would become increasingly slower with increasing reaction time. As shown in Fig. 2d and g, when the reaction time was extended to 10 h, a mixture of ZIF-8 and ZIF-L was obtained as the irregular ZIF-L with weak crystallinity was transformed into rhombic dodecahedral ZIF-8, and rod-like ZIF-L with better crystallinity was maintained using ethanol as the washing solvent. When the procedure continued for more than 15 h or even 24 h, only rod-like ZIF-L was obtained (Fig. 2h–j). The schematic diagram of the formation mechanism is shown in Fig. 3.

The functional groups of the ZIFs obtained in the presence of PVP with different reaction times were examined by FTIR spectroscopy. As shown in Fig. S4a and b,† the characteristic absorption peak of Zn–N stretching bands is observed at 418 cm^{-1}. The bands at 600–800 cm^{-1} and 900–1350 cm^{-1} are assigned to the out-of-plane and in-plane bending of the 2-mim ring, respectively.[16,40] The entire ring stretching of the imidazole is located at 1350–1500 cm^{-1}.[16,40] The spectral region of 2900–3200 cm^{-1} arises from the aliphatic and aromatic C–H stretching of 2-mim. The peak at 1565 cm^{-1} is associated with the N–H bending vibration of 2-mim (Fig. S4c and d†), while the peak at 2426 cm^{-1} can be assigned to the N–H···N hydrogen bond that bridges the ZIF-L layers (Fig. S4e and f†).[16] It can be clearly seen that in the presence of

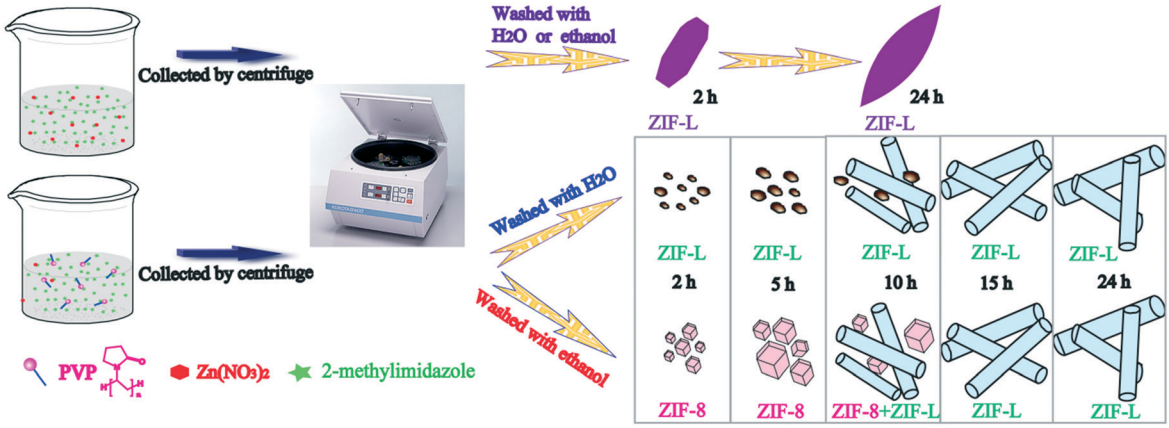

Fig. 3 Schematic diagram of the formation mechanism of leaf- and rod-like ZIF-L.

PVP, these two peaks (1565 cm^{-1} and 2426 cm^{-1}) did not appear when the reaction time was shorter than 10 h, but with increasing reaction time, the two peaks appeared, indicating that ZIFs with different coordination modes can be obtained in the presence of PVP when the reaction time is changed. However, the peaks at 1565 and 2426 cm^{-1} were always present for the ZIFs obtained at different reaction times without PVP, revealing that only ZIF-L was formed in the absence of PVP even though ethanol was used during the washing process. This corresponded well with the XRD and TEM results.

The structure transformation often follows two mechanisms: one is a solid-to-solid transformation mechanism that does not need liquid phase involvement; the other one is a dissolution–recrystallization mechanism, in which the solvent plays an important role in the process of crystallization.[39] To confirm the mechanism of the phase transformation evolved in this study, an experiment was conducted. In detail, ZIF(2h) prepared with PVP and washed with pure water was placed in a device, as shown in Fig. S5a.† The device was placed in an oven, and then heated at 80 °C for a period of time. ZIF-8 could also be obtained without liquid ethanol contact (Fig. S5d†), indicating that ZIF-L can be transformed into ZIF-8 in ethanol vapor *via* the solid-to-solid transformation mechanism.

From the above discussion, it can be concluded that a facile method to prepare both ZIF-8 and ZIF-L in aqueous solution was developed using ethanol as the washing solvent during the washing process in the presence of PVP when the ratio of 2-mim to $Zn(NO_3)_2$ was 10. In addition, nitrogen adsorption–desorption isotherms of ZIFs with different reaction times in the presence of PVP are shown in Fig. S6 and Table S1.† It could be seen that the specific surface area of ZIFs decreased with increasing reaction time because ZIF-8 has a much greater surface area than ZIF-L, and the size of the ZIFs increased gradually.

In summary, leaf-like ZIF-L and rod-like ZIF-L were facilely prepared from aqueous solutions of $Zn(NO_3)_2$/2-mim in the absence and presence of PVP, respectively. The formation of the leaf-like ZIF-L underwent nucleation and growth stages, while the rod-like ZIF-L was formed through a self-assembly mechanism. In the presence of PVP, the different washing solvents used to wash the products during their separation from the corresponding mother solution led to different outcomes within the first 10 h. In detail, when pure water and ethanol were used to wash the products, ZIF-L and ZIF-8 were obtained within 5 h, respectively. It was found that the phase transformation was controlled by both PVP and ethanol. PVP facilitated the nucleation of ZIF-L due to the weak interaction between Zn^{2+} and N atoms in PVP, resulting in the presence of a large amount of ZIF-L particles with weak crystallinity and small size, which contributed to the phase transformation when ethanol was introduced during the washing process. With this facile method, ZIFs with different morphologies, sizes and coordination modes can be obtained just by changing the reaction time.

Conflicts of interest

There are no conflicts to declare.

Acknowledgements

This work was supported by the National Natural Science Foundation of China (21575011, 51578034), the Beijing Talent Project (2017A38), the Great Wall Scholars Training Program Project of Beijing Municipality Universities (CIT&TCD20180323), and the Project of Construction of Innovation Teams and Teacher Career Development for Universities and Colleges Under Beijing Municipality (IDHT20170508).

Notes and references

1 N. Stock and S. Biswas, *Chem. Rev.*, 2012, **112**, 933.
2 Q. L. Zhu and Q. Xu, *Chem. Soc. Rev.*, 2014, **43**, 5468.
3 B. Chen, Z. Yang, Y. Zhu and Y. Xia, *J. Mater. Chem. A*, 2014, **2**, 16811.
4 R. Banerjee, A. Phan, B. Wang, C. Knobler, H. Furukawa, M. O'Keeffe and O. M. Yaghi, *Science*, 2008, **319**, 939.
5 F. Zhang, Y. Wei, X. Wu, H. Jiang, W. Wang and H. Li, *J. Am. Chem. Soc.*, 2014, **136**, 13963.

6 J. Yao and H. Wang, *Chem. Soc. Rev.*, 2014, **43**, 4470.
7 C. Chizallet, S. Lazare, D. Bazer-Bachi, F. Bonnier, V. Lecocq, E. Soyer, A. A. Quoineaud and N. Bats, *J. Am. Chem. Soc.*, 2010, **132**, 12365.
8 B. Wang, A. P. Côté, H. Furukawa, M. O'Keeffe and O. M. Yaghi, *Nature*, 2008, **453**, 207.
9 P. Z. Li, K. Aranishi and Q. Xu, *Chem. Commun.*, 2012, **48**, 3173.
10 Y. S. Li, F. Y. Liang, H. Bux, A. Feldhoff, W. S. Yang and J. Caro, *Angew. Chem., Int. Ed.*, 2010, **49**, 548.
11 K. S. Park, Z. Ni, A. P. Côté, J. Y. Choi, R. Huang, F. J. Uribe-Romo, H. K. Chae, M. O'Keeffe and O. M. Yaghi, *Proc. Natl. Acad. Sci. U. S. A.*, 2006, **103**, 27–10186.
12 S. R. Venna and M. A. Carreon, *J. Am. Chem. Soc.*, 2010, **132**, 76.
13 Y. Pan, Y. Liu, G. Zeng, L. Zhao and Z. Lai, *Chem. Commun.*, 2011, **47**, 207.
14 R. Chen, J. Yao, Q. Gu, S. Smeets, C. Baerlocher, H. Gu, D. Zhu, W. Morris, O. M. Yaghi and H. Wang, *Chem. Commun.*, 2013, **49**, 9500.
15 Y. R. Lee, M. S. Jang, H. Y. Cho, H. J. Kwon, S. Kim and W. S. Ahn, *Chem. Eng. J.*, 2015, **271**, 276.
16 Z. X. Low, J. Yao, Q. Liu, M. He, Z. Wang, A. K. Suresh, J. Bellare and H. Wang, *Cryst. Growth Des.*, 2014, **14**, 6589.
17 L. Hu, P. Zhang, Q. Chen, H. Zhong, X. Hu, X. Zheng, Y. Wang and N. Yan, *Cryst. Growth Des.*, 2012, **12**, 2257.
18 J. T. Zai, J. Zhu, R. R. Qi and X. F. Qian, *J. Mater. Chem. A*, 2013, **1**, 735.
19 T. Tong, A. Shereef, J. Wu, C. T. T. Binh, J. J. Kelly, J. F. Gaillard and K. A. Gray, *Environ. Sci. Technol.*, 2013, **47**, 12486.
20 T. Enomoto, S. Ueno, E. Hosono, M. Hagiwara and S. Fujihara, *CrystEngComm*, 2017, **19**, 2844.
21 C. Zhang, X. Wang, M. Hou, X. Li, X. Wu and J. Ge, *ACS Appl. Mater. Interfaces*, 2017, **9**, 13831.
22 J. Zhang, T. Zhang, K. Xiao, S. Cheng, G. Qian, Y. Wang and Y. Feng, *Cryst. Growth Des.*, 2016, **16**, 6494.
23 J. Yao, M. He and H. Wang, *CrystEngComm*, 2015, **17**, 4970.
24 A. Schejn, L. Balan, V. Falk, L. Aranda, G. Medjahdi and R. Schneider, *CrystEngComm*, 2014, **16**, 4493.
25 B. Motevalli, N. Taherfar, H. Wang and J. Z. Liu, *J. Phys. Chem. C*, 2017, **121**, 2221.
26 Z. X. Low, A. Razmjou, K. Wang, S. Gray, M. Duke, H. Wang and J. Membrane, *Sci.*, 2014, **460**, 9.
27 X. Li, Z. Li, L. Lu, L. Huang, L. Xiang, J. Shen, S. Liu and D. Xiao, *Chem. – Eur. J.*, 2017, **23**, 10638.
28 H. Jiang, S. Xue, Y. Liu, R. Chen and W. Xing, *RSC Adv.*, 2016, **6**, 21337.
29 H. Jiang, S. Xue, Y. Liu, W. Xing and R. Chen, *Microporous Mesoporous Mater.*, 2017, **243**, 16.
30 W. Han, H. Zhang, J. Chen, Y. Zhao, Q. Fan and Q. Li, *RSC Adv.*, 2015, **5**, 12605.
31 S. Xue, H. Jiang, Z. Zhong, Z. X. Low, R. Chen and W. Xing, *Microporous Mesoporous Mater.*, 2016, **221**, 220.
32 Y. Lo, C. H. Lam, C. W. Chang, A. C. Yang and D. Y. Kang, *RSC Adv.*, 2016, **6**, 89148.
33 C. Wang, E. Shen, E. Wang, L. Gao, Z. Kang, C. Tian, Y. Lan and C. Zhang, *Mater. Lett.*, 2005, **59**, 2867.
34 C. Ho, J. C. Yu, T. Kwong, A. C. Mak and S. Lai, *Chem. Mater.*, 2005, **17**, 4514.
35 G. D. Lilly, J. Lee, K. Sun, Z. Tang, K. S. Kim and N. A. Kotov, *J. Phys. Chem. C*, 2008, **112**, 370.
36 J. Zhang, F. Huang and Z. Lin, *Nanoscale*, 2010, **2**, 18.
37 M. J. Chen, A. C. Yang, N. H. Wang, H. C. Chiu, Y. L. Li, D. Y. Kang and S. L. Lo, *Microporous Mesoporous Mater.*, 2016, **236**, 202.
38 Z. Zhong, J. Yao, R. Chen, Z. Low, M. He, J. Z. Liu and H. Wang, *J. Mater. Chem. A*, 2015, **3**, 15715.
39 J. Zhang, T. Zhang, D. Yu, K. Xiao and Y. Hong, *CrystEngComm*, 2015, **17**, 8212.
40 M. Jian, B. Liu, R. Liu, J. Qu, H. Wang and X. Zhang, *RSC Adv.*, 2015, **5**, 48433.